Effects of localized spins on excitons in single-walled carbon nanotubes with imperfections

Satoru Konabe[1,2] **and Susumu Okada**[1,2]

[1]Graduate School of Pure and Applied Sciences, University of Tsukuba, 1-1-1 Tennodai, Tsukuba, Ibaraki 305-8571, Japan
[2]Japan Science and Technology Agency, CREST, 5 Sanbancho, Chiyoda, Tokyo 102-0075, Japan

E-mail: konabe@comas.frsc.tsukuba.ac.jp

Abstract. Excitons comprising of electron-hole pairs are one of representing many-body effects in carbon nanotubes (CNTs) and well known to affects optical properties of CNTs. Besides the excitons, another fascinating many-body effect in CNTs is magnetism that is inherent in CNTs with certain imperfections, such as adsorbents, defects, and interfaces, in their hexagonal atomic network. In the present study, we report the interesting interplay between these two many-body effects in CNTs: The localized spins originated from imperfections in CNTs can couple to the excitons and change the spin state of excitons. We show that the interaction can be written as the spin–spin interaction expressed by the Kondo-like Hamiltonian. Our calculation reveals that the interaction induces mixing between the singlet and triplet excitons and that this mixing produces optically activated triplet excitons. The results solves a recent mystery regarding the microscopic origin of unexpected behavior in the photoluminescence spectra of CNTs.

1. Introduction

In the past two decades, nanoscale carbon cylinders known as carbon nanotubes (CNTs) have been attracting great interest due to their unique physical properties that originate from their atomic network that has a quasi-one-dimensional honeycomb structure [1]. One of the fascinating properties of CNTs is the strong correlation between photoexcited carriers due to the enhanced Coulomb interaction caused by their one-dimensional structure. Consequently, photoexcited electrons and holes are strongly attracted to each other and form excitons that have binding energies of up to a few hundred millielectronvolts [2, 3, 4]. The high binding energies of these excitons are potentially valuable for studying fundamental excitonic physics and for utilizing CNTs in optoelectronic devices. Besides the excitons, another intriguing aspect of CNTs is the appearance of the spin polarization associated with modulation of the π electron network of CNTs due to imperfections such as defects, adatoms, and edges [5, 6, 7, 8, 9].

In this paper, we will unify these unique concepts in CNTs and show that the unification drastically changes the optical properties of CNTs, especially of the spin states of excitons. For this purpose, we develop a theory of excitons in defective CNTs. In this model, the defects are modeled in terms of polarized spins associated with localized states near the defects and an exciton then interacts with these localized spins. Using the tight-binding approximation, we calculate the absorption spectra by solving the Bethe–Salpeter equation. The primary result of the present work is that the triplet dark excitons become optically active by the exchange interaction between excitons and the localized spins at defect sites *without* the spin-orbit interaction. It is well known that the spin state of optically accessible excitons consists of the anti-parallel spins of a electron and hole pair, i.e., the singlet state, while optical excitation of excitons with the parallel spins, i.e., the triplet excitons, is forbidden by the spin selection rule for the materials with the weak spin-orbit interaction such as semiconducting CNTs. The model developed here may give rise to a new field of low-dimensional sciences for hybrid systems consisting of excitons and localized spins induced by defects.

2. Localized spins produced by vacancies and adatom impurities

We consider the polarized electron spins induced by defects, rather than the defects themselves. Defects such as vacancies and adatoms eliminate π electrons in the CNT, forming holes in the topological π network. CNTs have two kinds of atomic sites (i.e., they have a bipartite lattice) so that all atomic sites can be classified into one of two sublattices, A and B. Imperfections induce an imbalance between the numbers of these two carbon sublattice sites. Lieb's theorem states that bipartite networks possess a total electron spin S corresponding to the difference in the numbers of the two sublattices $S = (N_A - N_B)/2$ [10, 11, 12]. Early theoretical studies demonstrated that defects in π-network CNTs induce half-filled non-bonding electron states at the Fermi level [13] resulting in spin polarization near the Fermi level [5, 6, 7, 8, 9]. We thus expect that

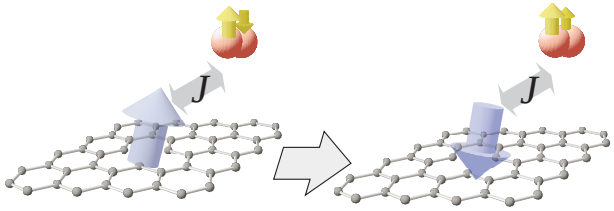

Figure 1. Schematic representation of the flipping process of exciton spins by the localized spin at the defect site. The localized spins around defects interact with excitons, resulting in mixing of singlet and triplet excitons.

these localized spins around defects interact with excitons resulting in mixing of singlet excitons and triplet excitons by flipping the spins of excitons (Fig. 1).

3. Interaction between excitons and localized spin

To derive the effective Hamiltonian for the interaction between an exciton and a localized spin, we start with the following Hamiltonian representing the exchange interaction between conduction (valence) electrons of excitons and the localized state at defect sites.

$$\mathcal{H}_{\rm ex} = -\sum_{m=c,v}\sum_{k,\sigma} J_m c^\dagger_{k_m,\sigma_m} c_{k'_m,\sigma'_m} f^\dagger_{i,\sigma'} f_{i,\sigma}\delta_{\sigma_m,\sigma}\delta_{\sigma'_m,\sigma'}, \tag{1}$$

where $c_{k_{c(v)},\sigma}$ is the annihilation operator for conduction (valence) electrons and $f_{i,\sigma}$ is the annihilation operator for a non-bonding state at a defect site i. σ indicates the up spin ($\uparrow$) and down spin ($\downarrow$). The exchange integral $J_{c(v)}$ is given by $J_{c(v)} \equiv \int d\mathbf{r}d\mathbf{r}'\ \psi^*_{\mathbf{k}_{c(v)}}(\mathbf{r})\phi^*_{\rm imp}(\mathbf{r}')v(\mathbf{r}-\mathbf{r}')\phi_{\rm imp}(\mathbf{r})\psi_{\mathbf{k}'_{c(v)}}(\mathbf{r}')$, where $\psi_{\mathbf{k}_{c(v)}}$is the wave function of the conduction (valence) bands and $\phi_{\rm imp}$ is the wave function of a non-bonding state at a defect site.

The exchange Hamiltonian Eq. (1) can be expressed in terms of the spin operators for conduction and valence electrons and for the localized non-bonding states:

$$\mathcal{H}_{\rm ex} = -\frac{J_c+J_v}{2}\sum_{kk'\sigma} c^\dagger_{k\sigma}c_{k'\sigma} - (J_c\boldsymbol{s}_c - J_v\boldsymbol{s}_v)\cdot\boldsymbol{S}, \tag{2}$$

where $\boldsymbol{s}_{c(v)} \equiv \sum_{k,k'}\sum_{\sigma,\sigma'} c^\dagger_{k,\sigma}\boldsymbol{\sigma}_{\sigma,\sigma'}c_{k',\sigma'}$ is the spin of conduction (valence) electrons and $\boldsymbol{S}$ is the spin of the localized state. $\boldsymbol{\sigma}$ are the Pauli matrices. This Hamiltonian consists of a spin-independent term (the first term) and a spin-dependent term (the second term). The latter term describes the exchange interaction between the spins of electrons or holes consisting of excitons and the localized spin, which we denote by $\mathcal{H}_{\text{ex-sp}}$:

$$\begin{aligned}\mathcal{H}_{\text{ex-sp}} = &\frac{S_+}{N}\sum_{k,k'}(J_c c^\dagger_{kc\downarrow}c_{k'c\uparrow} - J_v c^\dagger_{kv\downarrow}c_{k'v\uparrow}) \\ &+ \frac{S_-}{N}\sum_{k,k'}(J_c c^\dagger_{kc\uparrow}c_{k'c\downarrow} - J_v c^\dagger_{kv\uparrow}c_{k'v\downarrow})\end{aligned}$$

$$+\frac{S_z}{N}\sum_{k,k'}\Big[J_c(c^\dagger_{kc\uparrow}c_{k'c\uparrow}-c^\dagger_{kc\downarrow}c_{k'c\downarrow}) - J_v(c^\dagger_{kv\uparrow}c_{k'v\uparrow}-c^\dagger_{kv\downarrow}c_{k'v\downarrow})\Big]. \tag{3}$$

where $S_+ \equiv f^\dagger_\uparrow f_\downarrow$, $S_- \equiv f^\dagger_\downarrow f_\uparrow$, and $S_z \equiv (f^\dagger_\uparrow f_\uparrow - f^\dagger_\downarrow f_\downarrow)/2$. For convenience, we denote the first, second, and third terms of Eq. (3) as $\mathcal{H}^+_{\text{ex-sp}}$, $\mathcal{H}^-_{\text{ex-sp}}$, and $\mathcal{H}^z_{\text{ex-sp}}$, respectively. The Hamiltonian given in Eq. (3) is known as the Kondo exchange Hamiltonian. Recent advances in spintronics have revealed that this type of exchange interaction induces various interesting phenomena in optical devices including photoinduced magnetic order [14] and the optical RKKY interaction between localized spins [15].

4. Singlet-triplet mixing

Next, we investigate how the spin–spin interaction, Eq. (3), affects exciton states. We write exciton states as $|\alpha, \mathbf{K}\rangle$, where α denotes the spin singlet state or three triplet states and $\mathbf{K}$ denotes the momentum of the center of mass of the exciton. Using this notation, exciton states with finite momenta Q can be written as

$$|S,Q\rangle = \frac{1}{\sqrt{2}}\sum_q Z^S_{qc,(q-Q)v} \times (c^\dagger_{qc\uparrow}c_{(q-Q)v\uparrow}+c^\dagger_{qc\downarrow}c_{(q-Q)v\downarrow})|g\rangle, \tag{4}$$

$$|T_1,Q\rangle = \frac{1}{\sqrt{2}}\sum_q Z^{T_1}_{qc,(q-Q)v} \times (c^\dagger_{qc\uparrow}c_{(q-Q)v\uparrow}-c^\dagger_{qc\downarrow}c_{(q-Q)v\downarrow})|g\rangle, \tag{5}$$

$$|T_2,Q\rangle = \sum_q Z^{T_2}_{qc,(q-Q)v}c^\dagger_{qc\uparrow}c_{(q-Q)v\downarrow}|g\rangle, \tag{6}$$

$$|T_3,Q\rangle = \sum_q Z^{T_3}_{qc,(q-Q)v}c^\dagger_{qc\downarrow}c_{(q-Q)v\uparrow}|g\rangle, \tag{7}$$

where $|g\rangle$ is the vacuum for excitons. The exciton amplitudes $Z^n_{qc,(q-Q)v}$ in Eqs. (4)–(7) are obtained by solving the Bethe–Salpeter equation [2, 4, 16, 17]:

$$(\varepsilon_{\mathbf{k}_c}-\varepsilon_{\mathbf{k}_v})Z^n_{\mathbf{k}_c,\mathbf{k}_v}+\sum_{\mathbf{k}'_c,\mathbf{k}'_v}K_{\mathbf{k}'_c,\mathbf{k}'_v;\mathbf{k}_c,\mathbf{k}_v}Z^n_{\mathbf{k}'_c,\mathbf{k}'_v}=E^nZ^n_{\mathbf{k}_c,\mathbf{k}_v}, \tag{8}$$

where E^n is the exciton energy of the nth state and $K_{\mathbf{k}'_c,\mathbf{k}'_v;\mathbf{k}_c,\mathbf{k}_v}$ is the Coulomb interaction kernel that consists of exchange and screened-direct terms. The quasiparticle energy $\varepsilon_{\mathbf{k}_c}$ and the quasihole energy $\varepsilon_{\mathbf{k}_v}$ are calculated by applying the random-phase approximation [2, 16, 17]. For the Coulomb potential between π orbitals, we employed the Ohno potential $V(\mathbf{r}) = U/\kappa\sqrt{(\frac{4\pi\epsilon_0}{e^2}U|\mathbf{r}|)^2+1}$ with $U = 11.3$ eV [4, 16, 17]. The dielectric function $\kappa = 1.8$ for vacuum was chosen [18] to incorporate screening effects by σ bands and the surrounding environment. The calculations were performed under the tight-binding approximation taking nearest-neighbor hopping of 3.0 eV into account.

By the first-order perturbation on the spin–spin interaction of Eq. (3), the singlet

and triplet excitons become

$$|\tilde{S},0\rangle = |S,0\rangle + \sum_{i=1}^{3}\sum_{Q}|T_1,Q\rangle\frac{\langle T_1,Q|\mathcal{H}_{\text{ex-sp}}|S,0\rangle}{E_Q^{T_i}-E_0^S}, \tag{9}$$

$$|\tilde{T}_i,Q\rangle = |T_i,Q\rangle + |S,0\rangle\frac{\langle S,0|\mathcal{H}_{\text{ex-sp}}|T_i,Q\rangle}{E_0^S-E_Q^{T_i}}, \tag{10}$$

where E_0^S and $E_Q^{T_i}$ $(i=1,2,3)$ are the energies of the singlet and triplet excitons, respectively. As shown by the second terms in Eq. (9) and Eq. (10), a singlet exciton acquires a triplet character, whereas a triplet exciton acquires a singlet character.

The matrix elements of $\mathcal{H}_{\text{ex-sp}}$ for the singlet exciton state and three triplet exciton states with a momentum of Q, $|T_i,Q\rangle$ $(i=1,2,3)$ are derived as follows:

$$\langle T_1,Q|\mathcal{H}^z_{\text{ex-sp}}|S,0\rangle = \frac{JS_z}{N}\sum_k Z^{T_1*}_{(k+Q)c,kv}Z^S_{kc,kv}, \tag{11}$$

$$\langle T_{2(3)},Q|\mathcal{H}^{-(+)}_{\text{ex-sp}}|S,0\rangle = -\frac{(J_c+J_v)S_{-(+)}}{\sqrt{2}N}\sum_k Z^{T_{2(3)}*}_{(k+Q)c,kv}Z^S_{kc,kv}, \tag{12}$$

where we defined $J \equiv J_c - J_v$ as the difference between the exchange integrals. In these calculations, the localized spin $\boldsymbol{S}$ is treated as a classical spin. Although the spin selection rule permits the above matrix elements to have finite values, numerical calculations show that the matrix elements between the singlet and triplet excitons $\langle T_1,Q|\mathcal{H}_{\text{ex-sp}}|S,0\rangle$ have a non-zero value while the other matrix elements vanish for any finite Q. All the matrix elements are exactly zero by the orthogonality relation of the exciton wave function when the momentum of the triplet excitons is zero. Therefore, mixing occurs only between the singlet exciton $|S,0\rangle$ and the triplet exciton $|T_1,Q\neq 0\rangle$ by the spin–spin interaction under the condition, $J = J_c - J_v \neq 0$, which strictly holds for CNTs and other graphene-related materials. Hereafter, we use J as a control parameter to enable more general discussion of various polarized spin states induced by non-bonding states. The extent of these non-bonding states strongly depends on the shapes and sizes of the defects.

5. Absorption spectra

To calculate the absorption spectra, we need the matrix elements of the optical transition $W^S_{\text{ab}} \equiv \langle\tilde{S},0|\mathcal{H}_{\text{op}}|g\rangle$ and $W^{T_1}_{\text{ab}}(Q) \equiv \langle\tilde{T},Q|\mathcal{H}_{\text{op}}|g\rangle$ where $\mathcal{H}_{\text{op}}$ is the exciton–photon interaction [19]. These are calculated using the perturbed states derived from Eqs. (9) and (10):

$$W^S_{\text{ab}} = \sum_k Z^S_{kc,kv}\frac{D_k}{E_0^S}, \tag{13}$$

$$W^{T_1}_{\text{ab}}(Q) = JS_z\sum_k\frac{Z^{T_1*}_{(k+Q)c,kv}Z^S_{kc,kv}}{E_0^S-E_Q^{T_1}}\sum_q\frac{D_qZ^{S*}_{qc,qv}}{E_0^S}, \tag{14}$$

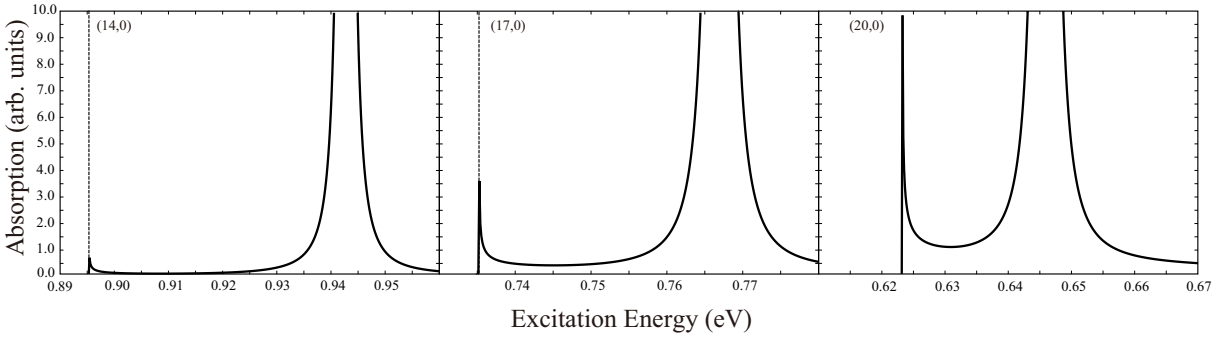

Figure 2. Absorption spectra of $(14,0)$, $(17,0)$, and $(20,0)$ CNTs. The exchange energy is $J = J_c - J_v = 5$ meV and the defect concentration is $c = 5\%$. The dashed line indicates the triplet exciton energy. Broadening is set to 1 meV.

where $D_{\mathbf{k}_c,\mathbf{k}_v} = \langle \mathbf{k}_c | z | \mathbf{k}_v \rangle$ is the dipole matrix element between the conduction and valence bands. The polarization axis of the laser beam is set to be parallel to the CNT axes (i.e., the z-axis) because this polarization configuration maximizes the optical absorption of the laser beam by the CNTs.

Without the mixing mechanism between singlet and triplet excitons, only the singlet exciton has a finite probability for the optical transition in Eq. (13). However, due to the spin–spin interaction, the perturbed triplet exciton has the singlet component represented by the second term in Eq. (10) and it can couple to the ground state by the exciton–photon interaction. Thus, the triplet dark exciton becomes optically allowed. This is analogous to the mechanism for the appearance of phonon side bands [20, 21]. In this case, the exciton–phonon interaction connects a bright exciton with zero momentum to a dark exciton with finite momentum, making the finite-momentum exciton optically active.

Using Eqs. (13) and (14), the absorption spectrum is given by:

$$\alpha(\hbar\omega) \propto \left|W_{\rm ab}^{S}\right|^2 \delta(\hbar\omega - E^S) + \sum_{Q} \left|W_{\rm ab}^{T_1}(Q)\right|^2 \delta(\hbar\omega - E_Q^{T_1}), \tag{15}$$

where $\hbar\omega$ is the photon energy. The first term originates from the optical transition of the singlet exciton and the second term is due to the triplet exciton intermediated by the singlet exciton. For the second term in Eq. (15), we should use the average impurity position and the average localized spin direction by assuming paramagnetism. This gives the factor $cS_z^2 = cS(S+1)/3$, where c is the defect concentration.

Figure 2 shows the calculated absorption spectra for $(14,0)$, $(17,0)$, and $(20,0)$ CNTs for $J = 5$ meV, $S = 1/2$, and a defect concentration of $c = 5\%$. These spectra clearly show the triplet exciton peak regardless of diameter of CNTs in addition to the singlet main peak. An optical transition between the ground and triplet states is possible through the singlet state in the perturbed triplet state $|\tilde{T}_1, Q\rangle$. The satellite peak is asymmetric because triplet excitons with finite momenta that exceed the bottom

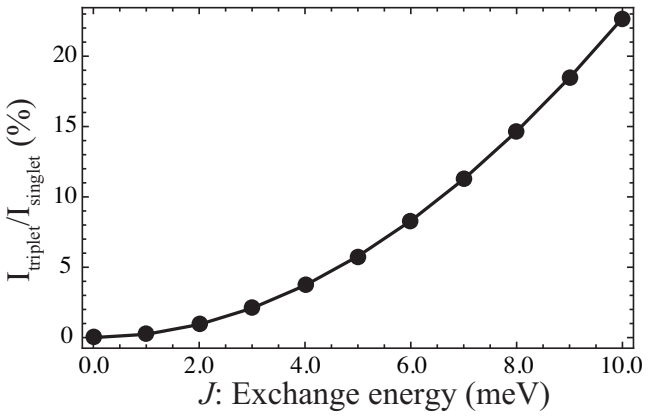

Figure 3. Spectral weight transfer of $(20, 0)$ CNTs as a function of $J = J_c - J_v$. The defect concentration is set to $c = 5\%$.

of the energy band are excited. This asymmetric spectral shape differs from those for the CNTs with the enhanced spin-orbit interaction or the encapsulated ferromagnets, whose spectral shapes are symmetric [22, 23]. We also calculated the ratio of the spectral weight $I_{\rm triplet}/I_{\rm singlet}$ for $(20, 0)$ CNTs as a function of J (see Fig. 3). This result shows that the spectral weight of the triplet exciton exceeds 20 % when $J = 10$ meV and $c = 5$ %. The spectral weight varies linearly with the defect concentration and the calculated results can be fitted by the phenomenological expression: $I_{\rm triplet}/I_{\rm singlet}(\%) \simeq 0.0023cJ^2$.

6. Discussion

The theory proposed in the present work resolves the recent outstanding problem regarding the satellite peak observed by photoluminescence (PL) experiments. PL measurements using high-intensity laser irradiation [24, 25] or atomic hydrogen exposure [26] have revealed the presence of a satellite peak in addition to the main peak of the spin-singlet bright exciton. Based on experimental studies, these satellite peaks have been ascribed to triplet dark excitons, which neither absorb nor emit light in pristine CNTs. The experiments show that the photoactive triplet excitons are commonly generated regardless of defect types so that this indicates the underlying universal physics that makes the triplet dark excitons optically allowed in defective CNTs. The theory developed in the present paper can be used for explaining all the experimental results since the theory covers both vacancies generated by high-intensity laser irradiation [24, 25] and adatoms produced by atomic hydrogen exposure [26], which are equivalent to each other from the topology of the π-network.

7. Conclusions

In summary, we have studied the optical properties of CNTs in terms of the effective interaction between excitons and localized spin near defects that are inherent in one-

dimensional bipartite networks. Our analysis is based on a model Hamiltonian and provides a unified theory for the microscopic mechanism for optical activation of triplet dark excitons. The satellite peak is attributed to the triplet exciton and it appears in the absorption spectra due to mixing between the singlet and triplet exciton states by the spin–spin interaction. Our calculation not only solves a recent important problem in the optical properties of CNTs but it also extends our understanding of many-body physical phenomena caused by the interaction between excitons and localized spins that are inherent in low-dimensional materials such as CNTs.

Acknowledgments

The authors thank Y. Homma, S. Chiashi, M. Arikawa and Y. Takagi for fruitful discussions. This work was supported by CREST in the Japan Science and Technology Agency and a Grant-in-Aid for Scientific Research from the Ministry of Education, Culture, Sports, Science and Technology (MEXT) of Japan.

References

[1] A. Jorio, G. Dresselhaus, and M. S. Dresselhaus, *Carbon Nanotubes: Advanced Topics in the synthesis, structure, properties and applications* (Spinger, Heidelberg, 2008).
[2] T. Ando, J. Phys. Soc. Jpn. **66**, 1066 (1997).
[3] C. D. Spataru, S. Ismail-Beigi, L. X. Benedict, and S. G. Louie, Phys. Rev. Lett. **92**, 077402 (2004).
[4] V. Perebeinos, J. Tersoff, and P. Avouris, Phys. Rev. Lett. **92**, 257402 (2004).
[5] S. Okada and A. Oshiyama, Phys. Rev. Lett. **87**, 146803 (2001).
[6] S. Okada and A. Oshiyama, J. Phys. Soc. Jpn. **72**, 1510 (2003).
[7] P. O. Lehtinen, A. S. Foster, A. Ayuela, T. T. Vehviläinen, and R. M. Nieminen, Phys. Rev. B **69**, 155422 (2004).
[8] Y. Ma, P. O. Lehtinen, A. S. Foster, and R. M. Nieminen, New. J. Phys. **6**, 68 (2004).
[9] Y. Ma, P. O. Lehtinen, A. S. Foster, and R. M. Nieminen, Phys. Rev. B **72**, 085451 (2005).
[10] H. C. Longuet-Higgins, J. Chem. Phys. **18**, 265 (1950).
[11] A. A. Ovchinnikov, Theoret. Chim. Acta **47**, 297 (1978).
[12] E. Lieb, Phys. Rev. Lett. **62**, 1201 (1989).
[13] M. Igami, T. Nakanishi, and T. Ando, J. Phys. Soc. Jpn. **68**, 3146 (1999).
[14] H. Ohno, Science **281**, 951 (1998).
[15] C. Piermarocch, P. Chen, L. J. Sham, and D. G. Steel, Phys. Rev. Lett. **89**, 167402 (2002).
[16] T. Ando, J. Phys. Soc. Jpn. **75**, 024707 (2006).
[17] J. Jiang, R. Saito, Ge. G. Samsonidze, A. Jorio, S. G. Chou, G. Dresselhaus, and M. S. Dresselhaus, Phys. Rev. B **75**, 035407 (2007).
[18] R. B. Capaz, C. D. Spataru, S. Ismail-Beigi, and S. G. Louie, Phys. Status Solidi B **244**, 4016 (2007).
[19] J. Jiang, R. Saito, K. Sato, J. S. Park, Ge. G. Samsonidze, A. Jorio, G. Dresselhaus, and M. S. Dresselhaus, Phys. Rev. B **75**, 035405 (2007).
[20] V. Perebeinos, J. Tersoff, and P. Avouris, Phys. Rev. Lett. **94**, 027402 (2005).
[21] O. N. Torrens, M. Zheng, and J. M. Kikkawa, Phys. Rev. Lett. **101**, 157401 (2008).
[22] S. Konabe and K. Watanabe, Phys. Rev. B **83**, 045407 (2011).
[23] S. Konabe and S. Okada, Appl. Phys. Lett. **98**, 073109 (2011).

[24] H. Harutyunyan, T. Gokus, A. A. Green, M. C. Hersam, M. Allegrini, and A. Hartschuh, Nano Lett. **9**, 2010 (2009).
[25] R. Matsunaga, K. Matsuda, and Y. Kanemitsu, Phys. Rev. B **81**, 033401 (2010).
[26] K. Nagatsu, S. Chiashi, S. Konabe, and Y. Homma, Phys. Rev. Lett. **105**, 157403 (2010).